

Accepted Manuscript

Silver complexes with sulfathiazole and sulfamethoxazole: synthesis, spectroscopic characterization, crystal structure and antibacterial assays

Julia Helena Bormio Nunes, Raphael Enoque Ferraz de Paiva, Alexandre Cuin, Wilton Rogério Lustrri, Pedro Paulo Corbi

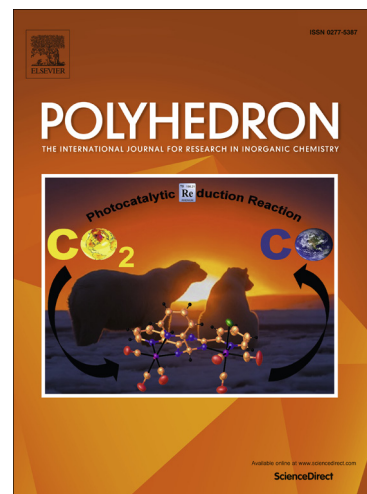
PII: S0277-5387(14)00613-5
DOI: <http://dx.doi.org/10.1016/j.poly.2014.09.010>
Reference: POLY 10975

To appear in: *Polyhedron*

Received Date: 7 July 2014
Accepted Date: 11 September 2014

Please cite this article as: J.H.B. Nunes, R.E.F. de Paiva, A. Cuin, W.R. Lustrri, P.P. Corbi, Silver complexes with sulfathiazole and sulfamethoxazole: synthesis, spectroscopic characterization, crystal structure and antibacterial assays, *Polyhedron* (2014), doi: <http://dx.doi.org/10.1016/j.poly.2014.09.010>

This is a PDF file of an unedited manuscript that has been accepted for publication. As a service to our customers we are providing this early version of the manuscript. The manuscript will undergo copyediting, typesetting, and review of the resulting proof before it is published in its final form. Please note that during the production process errors may be discovered which could affect the content, and all legal disclaimers that apply to the journal pertain.



1
2
3
4
5
6
7
8
9
10
11
12
13
14
15
16
17
18
19
20
21
22
23
24
25
26
27
28
29
30
31
32
33
34
35
36
37
38
39
40
41
42
43
44
45
46
47
48
49
50
51
52
53
54
55
56
57
58
59
60
61
62
63
64
65

Silver complexes with sulfathiazole and sulfamethoxazole: synthesis, spectroscopic characterization, crystal structure and antibacterial assays

Julia Helena Bormio Nunes,^a Raphael Enoque Ferraz de Paiva,^a Alexandre Cuin,^b

Wilton Rogério Lustri^c and Pedro Paulo Corbi^{a*}

^a *Bioinorganic and Medicinal Chemistry Research Laboratory, University of Campinas – UNICAMP PO Box 6154, 13083-970, Campinas – SP, Brazil*

^b *Bioinorganic Chemistry Research Laboratory, Federal University of Juiz de Fora, 36036-330, Juiz de Fora - MG, Brazil*

^c *Biological and Health Sciences Department – UNIARA, 14801-320 Araraquara, SP, Brazil*

This work is dedicated to Professor Antonio Carlos Massabni in the occasion of his 70th anniversary.

*Corresponding author:

Institute of Chemistry – University of Campinas.

PO Box 6154, 13083-970, Campinas, SP, Brazil

Telephone: + 5519 35213130 / FAX: + 5519 35213023

E-mail addresses: ppcorbi@iqm.unicamp.br

Abstract

The present work describes the synthesis and spectroscopic characterization of two silver(I) complexes with the sulfonamides sulfathiazole ($\text{AgC}_9\text{H}_8\text{N}_3\text{O}_2\text{S}_2$, Ag-SFT) and sulfamethoxazole ($\text{AgC}_{10}\text{H}_{10}\text{N}_3\text{O}_3\text{S}$, Ag-SFM). Elemental analyses indicate a 1:1 metal/ligand composition for both complexes. Spectroscopic techniques such as ^1H , ^{15}N NMR and IR evidence the coordination of both ligands to silver through the nitrogen atom of the sulfonamide group, and also indicate the participation of the 5-membered N-heterocyclic ring in the coordination. The Ag-SFT crystal structure was solved by X-ray powder diffraction and indicates the formation of a dimeric structure with silver bridging between two ligand molecules. Biological studies showed the antibacterial activity of Ag-SFT and Ag-SFM complexes against Gram-positive and Gram-negative bacterial strains, with MIC values ranging from 3.45-6.90 mmol L^{-1} for the sulfathiazole complex and 1.74-13.9 mmol L^{-1} for the sulfamethoxazole complex. The complexes have shown to be more active against Gram-negative bacterial strains.

Keywords: Sulfathiazole; Sulfamethoxazole; Silver; X-ray diffraction; NMR; Antibacterial agents.

Abbreviations list (in alphabetical order)

1
2 Ag-SFM – Ag(I) complex with sulfamethoxazole
3

4 Ag-SFT – Ag(I) complex with sulfathiazole
5

6
7 CFU – Colony-forming units
8

9 DMSO – Dimethylsulfoxide
10

11 IR – Infrared vibrational spectroscopy
12

13 MIC – Minimum inhibitory concentration
14

15 NMR – Nuclear magnetic resonance
16

17 SFM – Sulfamethoxazole
18

19 SFT – Sulfathiazole
20

21 UV-Vis – Ultraviolet-visible electronic spectroscopy
22
23
24
25
26
27
28
29
30
31
32
33
34
35
36
37
38
39
40
41
42
43
44
45
46
47
48
49
50
51
52
53
54
55
56
57
58
59
60
61
62
63
64
65

Introduction

The applications of silver compounds as antimicrobial agents started with the use of silver nitrate in the middle-ages. At that time, such compound was used to cure skin infections [1]. In the 1960's, silver sulfadiazine was synthesized. It was the first silver sulfonamide based drug used in the treatment of burns in order to prevent skin infections [1,2]. Since then, new silver-based compounds have been synthesized in order to obtain new antibiotics safer and more efficient to different pathogenic microorganisms. Due to its multi-targeting mechanism, silver-based antimicrobial agents are often capable to overcome bacterial resistance. Silver(I) has shown to be able to inactivate proteins, bind to thiol groups and form stable Ag-S bonds. Silver can also take part in catalytic redox reactions, resulting in the formation of disulfide bonds (R-S-S-R). The formation of disulfide bonds can lead to alterations in the protein secondary and tertiary structures, leading to inactivation of key enzymes, and also block respiration and electron transfer. It was also found that silver binds to DNA. Modak and Fox studied the exposition of *Pseudomonas aeruginosa* to sub lethal doses of silver sulfadiazine and observed that up to 12% of the silver appears bound to the DNA [3]. Silver(I) enters the cell through transmembrane proteins. The protein CopB-ATPase from *Enterococcus hirae*, for example, is capable to mediate the silver ion transport, although its putative function is copper transport [4]. Silver ions are also able to change the structure of the bacteria cell wall, leading to changes in its mobility and stability and to a subsequent bacterial death [5-7]. A recent review was published by Eckhardt et al. dealing with some of the biological aspects of silver-containing materials (complexes with amino acids and peptides, composites and nanoparticles) and mechanisms of action and resistance [8]. More recently, Kyros et al. described new silver complexes with N,S donor ligands, such as $[AgCl(TPP)_2(MTZD)]$. This compound have shown to possess

1
2
3
4
5
6
7
8
9
10
11
12
13
14
15
16
17
18
19
20
21
22
23
24
25
26
27
28
29
30
31
32
33
34
35
36
37
38
39
40
41
42
43
44
antibacterial activities against *P. aeruginosa* and *E. coli* bacterial strains, with a MIC value of 40 $\mu\text{mol L}^{-1}$ [9].

Historically, sulfonamides were the first effective chemotherapeutic agents employed systematically for the prevention and treatment of bacterial infections in humans [10]. They are a group of bacteriostatic drugs that act by competitive inhibition of PABA (para-aminobenzoic acid), a co-factor required for bacterial synthesis of folic acid [11]. The development of new metal complexes with sulfonamides is an important field of research, considering that one can combine the specific antibacterial activities of the sulfonamides and the multi-targeting antimicrobial activities of the metal ions. In many cases, the metal complex exhibits a better activity than the free ligand [12]. As reported, silver sulfadiazine was the first silver sulfonamide compound developed. It is an efficient topical compound for reducing the development of early burn-sound sepsis. Silver sulfadiazine was at least 50 times more active than sulfadiazine alone. Other benefits of using silver sulfadiazine over silver nitrate are the low tendency to remove chloride ions, extended inhibition effect over time, lesser corrosive effect and activity against both Gram-positive and Gram-negative bacteria [13]. Nevertheless, silver sulfadiazine has shown to be insoluble in water and in other common organic solvents, which limits its application in medicine.

45
46
47
48
49
50
51
52
53
54
55
56
57
58
59
60
61
62
63
64
65
Sulfathiazole (SFT) was one of the first sulfonamides used in humans after the discovery of the sulfa drugs. Due to its high toxicity, it is used with other sulfonamides such as sulfabenzamide and sulfacetamide in preparations for the topical treatment of vaginal infections. It is also used combined to other drugs in the treatment of skin infections [14]. Many metal complexes of sulfathiazole are reported in the literature. Some examples are the cobalt(II) complexes with sulfathiazole, which presents

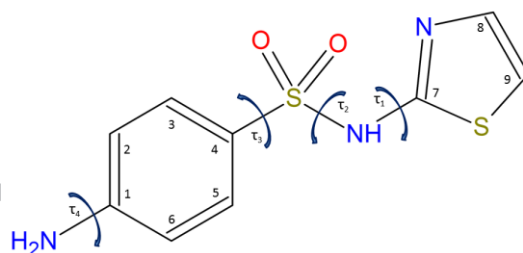
1 activities against *Aspergillus fumigatus* and *Aspergillus flavus* [15,16]. Also, a
2 platinum(II) complex of sulfathiazole, *cis*-[Pt(STZ)₂(PPh₃)₂], in which the sulfathiazole
3 ligands coordinate via the nitrogen atoms of the thiazole ring [17], and a former silver(I)
4 complex of sulfathiazole, which was synthesized and characterized solely by infrared
5 and electronic spectroscopies, were reported earlier [18]. Although the silver complex
6 of sulfathiazole has already been described, it was not fully characterized and no
7 biological studies have been conducted yet. The structure of sulfathiazole with carbon
8 assignments is shown in Fig. 1-A
9

10
11
12
13
14
15
16
17
18
19
20 Sulfamethoxazole (SFM) was part of the second generation of sulfonamides.
21
22 Nowadays it is used in a synergistic combination with trimethoprim. Sulfamethoxazole
23 is also the drug of choice to treat infections produced by *Pneumocystis pneumonia*,
24 which is a form of pneumonia caused by a yeast-like fungus that affects patients with
25 HIV [19]. There are also some metal complexes of sulfamethoxazole reported in the
26 literature. A cobalt(II) complex of sulfamethoxazole was obtained, and the X-ray
27 diffraction studies showed that the metal in [Co(sulfamethoxazole)₂(H₂O)₂]₂H₂O is in a
28 slightly distorted octahedral environment, with sulfamethoxazole molecules acting as
29 head-to-tail bridges between two cobalt atoms, forming polymeric chains. The
30 microbiological assays against *M. tuberculosis* showed that the complex was not able to
31 permeate through the mycobacteria cell wall [20]. In addition, cobalt(II) and
32 cadmium(II) complexes of sulfamethoxazole had their infrared spectra investigated. In
33 the cadmium complex, the ligand binds to the metal through the nitrogen and oxygen
34 atoms of the sulfonamide, while in the cobalt compound the metal coordinates through
35 the sulfonamide and amino nitrogen atoms [21]. Also, gold(I) and silver(I) complexes
36 of sulfamethoxazole were earlier synthesized and characterized by X-ray diffraction.
37
38
39
40
41
42
43
44
45
46
47
48
49
50
51
52
53
54
55
56
57
58
59
60
61
62
63
64
65

1 nitrogen of the sulfonamide group. The same coordination mode is observed for the
2 silver(I) complex. Both compounds were tested against Gram-positive and Gram-
3 negative bacteria, and the gold complex showed greater activity against *E. coli* and *S.*
4 *aureus* than the silver one [22]. The structure of sulfamethoxazole with carbon
5 assignments is shown in Fig. 1-B.
6
7
8
9
10

11
12 The present work brings a complete study on synthesis, spectroscopic
13 characterization and antibacterial assays over Gram-positive and Gram-negative
14 pathogenic bacterial strains of silver(I) complexes with sulfathiazole and
15 sulfamethoxazole. A new crystal structure for the silver-sulfathiazole complex is also
16 reported here.
17
18
19
20
21
22
23
24
25
26

27 **A**



51 **B**

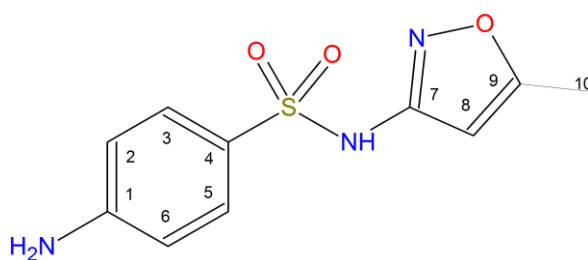


Fig. 1. Sulfathiazole (A) and sulfamethoxazole (B) structures with carbon numbering. The four torsion angles used in the powder diffraction studies were assigned in the SFT drawn.

Experimental

Materials

Sulfathiazole, sulfamethoxazole, potassium hydroxide and silver(I) nitrate were from Sigma-Aldrich Laboratories (purity >98%).

Equipment

Elemental analyses for carbon, hydrogen and nitrogen were performed using a Perkin Elmer 2400 CHNS/O Analyzer. Infrared (IR) spectra were measured in KBr pellets using a Bomem MB-Series Model B100 FT-IR spectrophotometer in the range 4000-400 cm^{-1} with resolution of 4 cm^{-1} . Solution-state ^1H , $^{13}\text{C}\{^1\text{H}\}$ NMR and the [^1H - ^{15}N] correlation nuclear magnetic resonance spectra were recorded on a Bruker Avance III 500 MHz. Samples were analyzed in deuterated dimethylsulfoxide- d_6 solutions and the chemical shifts were given relative to tetramethylsilane (TMS). Mass spectra were obtained on a Waters Quattro Micro API with direct infusion and operating in the negative mode. Samples of the complexes were prepared DMSO and further diluted 100-fold in methanol. The UV-Vis spectra were recorded in $9.90 \times 10^{-6} \text{ mol L}^{-1}$ to $4.76 \times 10^{-6} \text{ mol L}^{-1}$ DMSO solutions using 10.00 mm quartz cuvettes in a Hewlett-Packard 8453A diode array spectrophotometer.

Synthesis of Ag-SFT

The silver(I) complex with sulfathiazole (Ag-SFT) was synthesized by the reaction of 7.0 mL of an aqueous solution containing $5.0 \times 10^{-4} \text{ mol}$ (0.1279 g) of the sulfathiazole (SFT) and $1.0 \times 10^{-3} \text{ mol}$ (0.0549 g) of KOH with 2.0 mL of an aqueous solution containing $5.0 \times 10^{-4} \text{ mol}$ (0.0854 g) of AgNO_3 . The synthesis was carried out with stirring at room temperature. After one hour, the white solid obtained was vacuum

1 filtered, washed with cold water and dried in a desiccator under vacuum. Anal. Calc.
2 for $\text{AgC}_9\text{H}_8\text{N}_3\text{O}_2\text{S}_2$ (%): C, 29.6 ; H, 2.76 ; N, 11.5. Found (%): C, 29.5; H, 2.30 ; N,
3
4 11.4. The yield of the synthesis was 90%. The Ag-SFT is insoluble in dichloromethane,
5 chloroform, acetonitrile, hexane, acetone, ethanol, methanol and water. It is soluble in
6
7 DMSO and is stable in this solvent. The Ag-SFT complex shows a band centered at 290
8
9 nm in the UV-Vis spectrum with molar absorptivity coefficient of $15210 \text{ L mol}^{-1} \text{ cm}^{-1}$ in
10
11 DMSO.
12
13
14
15

16 17 18 19 *Synthesis of Ag-SFM*

20
21 The silver(I) complex with sulfamethoxazole (Ag-SFM) was synthesized by the
22 reaction of 5.0 mL of an aqueous solution containing 4.0×10^{-4} mol (0.1015 g) of the
23 sulfamethoxazole (SFM) and 8.0×10^{-4} mol (0.0476 g) of KOH with 1.0 mL of an
24 aqueous solution containing 4.0×10^{-4} mol (0.0685 g) of AgNO_3 . The synthesis was
25 carried out with stirring at room temperature. After one hour a white solid obtained was
26 vacuum filtered, washed with cold water and dried in a desiccator under vacuum. Anal.
27 Calc. for $\text{AgC}_{10}\text{H}_{10}\text{N}_3\text{O}_3\text{S}$ (%): C, 33.3 ; H, 2.80 ; N, 11.7. Found (%): C, 32.1; H, 2.86;
28 N, 11.1. The yield of the synthesis was 70%. As observed for the Ag-SFT complex, the
29 Ag-SFM is insoluble in dichloromethane, chloroform, acetonitrile, hexane, acetone,
30 ethanol, methanol and water. It is also soluble and stable in DMSO. The UV-Vis
31 spectrum of Ag-SFM complex shows a band centered at 269 nm with a molar
32 absorptivity coefficient of $19874 \text{ L mol}^{-1} \text{ cm}^{-1}$ in DMSO.
33
34
35
36
37
38
39
40
41
42
43
44
45
46
47
48
49
50
51
52

53 *Structural analysis of Ag-SFT by X-ray powder diffraction*

54
55 A polycrystalline sample of Ag-STF was manually ground in an agate mortar
56 and then deposited in the hollow of a PMMA sample holder equipped with low
57
58
59
60
61
62
63
64
65

1 background plate. The diffraction data were collected on a Bruker Axs D8 da Vinci
2 equipment using CuK_α (1.5418 Å) radiation; the generator was operated at 40 kV and
3
4 40 mA. The diffractometer was equipped with a Ni filter and a linear position sensitive
5
6 detector (PSD), with the following optics: primary beam soller slits 2.94 °, fixed
7
8 divergence slit at 0.3 °; receiving slit 8 mm. Since indexing seemed viable, scans were
9
10 performed in the 5-105 ° 2θ range for 5 hours, with step of 0.02 °. Indexing was
11
12 performed with the aid of the single value decomposition approach as implemented in
13
14 the TOPAS-R suite of programs [TOPAS-R (Version 4.2), Bruker AXS, Karlsruhe,
15
16 Germany (2009)]. The space group $P2_1/c$ was assigned on the basis of the systematic
17
18 extinction conditions and confirmed by successful structure solutions and refinements.
19
20 Structure solution was performed by using the simulated annealing technique also
21
22 implemented in TOPAS-R, with the organic moieties treated as rigid bodies idealized as
23
24 Z-matrix where torsion angles τ_1 to τ_3 were left free and Ag(I) ion was “freely floating”.
25
26 The final Rietveld refinement plots are shown in Electronic Supplementary Information
27
28 (ESI) #1. The refinement was performed by the Rietveld method using TOPAS-R,
29
30 freeing all torsional angles described in Fig. 1A. Preferred orientation was refined in the
31
32 [100]. The experimental background was fit by a polynomial description. Silver was
33
34 given a refinable isotropic displacement parameter (BM), while lighter atoms were
35
36 assigned a common $B = \text{BM} + 2.0 \text{ \AA}^2$ value. Scattering factors corrected for real and
37
38 imaginary anomalous dispersion terms were taken from the internal library of TOPAS-
39
40 R. Final R_p , R_{wp} , R_{Bragg} and details on data collections and analyses can be found in
41
42 Table 1. The main bond distances and angles can be found in Table 2.
43
44
45
46
47
48
49
50
51
52
53
54
55
56
57
58
59
60
61
62
63
64
65

Antibacterial Assays

1
2
3 Three pathogenic bacterial strains, *S. aureus* ATCC 25923, *P. aeruginosa* ATCC
4 27853, and *S. enterica* ATCC 10708 were selected. Solutions and suspensions of SFT,
5 SFM, Ag-SFT and Ag-SFM were prepared in DMSO (20.0 mg mL⁻¹). Sufficient inocula
6 of the bacterial strains were added to a 96 multiwall plate until the turbidity equaled 1.0
7 McFarland (~3.0 x 10⁸ CFU mL⁻¹). The tested compounds were sequentially diluted into
8 the multiwall plate. A negative control was obtained by leaving one of the wells of each
9 bacterial strain with no addition of the considered compounds, only in DMSO, while the
10 silver nitrate was used as a positive control. The minimal inhibitory concentrations
11 (MIC) were estimated following the recommendations of the Clinical and Laboratory
12 Standards Institute (CLSI) [23]. All assays were performed in triplicate.
13
14
15
16
17
18
19
20
21
22
23
24
25
26
27
28
29
30

Results and Discussion

Crystal Structure Studies

31
32
33
34
35
36
37 The crystal structure of the Ag-SFM complex was previously elucidated by
38 Marques *et al.* [22] by a single-crystal analysis and showed the coordination of the
39 silver ion through the nitrogen of the sulfonamide group. Here, we have elucidated the
40 crystal structure of Ag-SFT by the state-of-art powder X-ray diffraction. The dimer of
41 Ag-SFT is shown in Fig. 2 where the atoms of asymmetric unit were labeled.
42
43
44
45
46
47
48
49
50
51
52
53
54
55
56
57
58
59
60
61
62
63
64
65

Table 1. Crystal Parameters of Ag-SFT

Ag-SFT	
Empirical formula	C ₉ H ₈ AgN ₃ O ₂ S ₂
Formula weight (g mol ⁻¹)	361.99
T(K)	298
λ(CuKα) (Å)	1.5418
Crystal System	Monoclinic
Space Group	P2 ₁ /c
a (Å)	13.1478(8)
b (Å)	5.4977(4)
c (Å)	16.0251(1)
β (°)	110.406(4)
V (Å ³)	1085.6(1)
Z	4
d _{calc} (g cm ⁻³)	2.2159(2)
μ (mm ⁻¹)	18.53
F(000)	712
Number of Parameters	30
R _p , R _{wp} , R _{Bragg}	0.066, 0.091, 0.046

Table 2. Selected distances and angles for Ag-SFT complex

Distance / Å		Angle / degree	
Ag-N1	2.120(2)	N2-Ag-N1	170.57(2)
Ag-N2	2.184(1)	N1-Ag-O2	77.56(6)
Ag-O1	2.579(2)	N2-Ag-O2	109.18(6)
Ag...Ag	2.895(6)		
Ag...O2	3.162(1)		

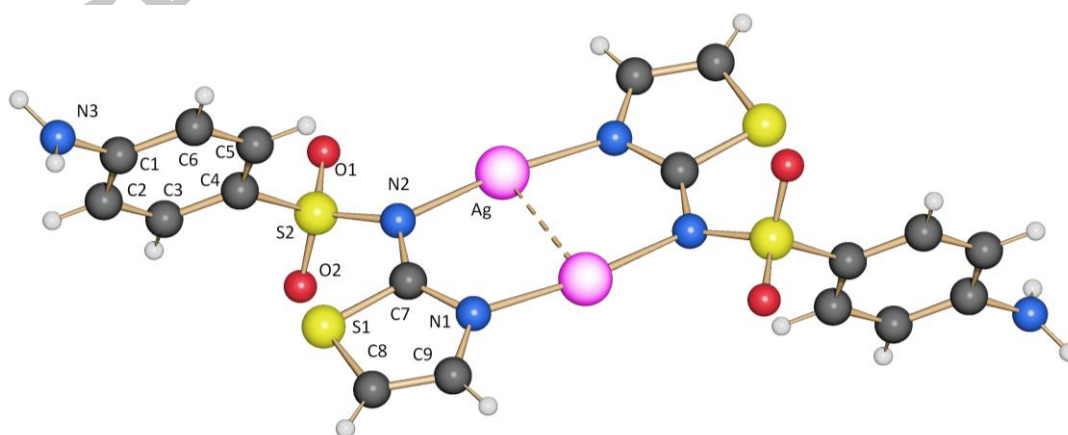


Fig. 2. Schakal [24] drawn of dimeric Ag-SFT. The atoms of the asymmetric unit of Ag-SFT are numbered and the symmetry code 2-x, 1-y, -z was applied to generate the dimer form. Silver is colored as pink; nitrogen, oxygen, sulfur, carbon and hydrogen atoms are colored as blue, red, yellow, black and white, respectively.

1
2
3
4
5
6
7
8
9
10
11
12
13
14
15
16
17
18
19
20
21
22
23
24
25
26
27
28
29
30
31
32
33
34
35
36
37
38
39
40
41
42
43
44
45
46
47
48
49
50
51
52
53
54
55
56
57
58
59
60
61
62
63
64
65

The Ag-SFT shows argentophilic interaction with the Ag...Ag distance 2.89 Å, as shown previously for Ag(I) complexes with carboxylic ligands [25, 26]. The dimer can be described as a centrosymmetric structure with an inversion center in the middle of Ag...Ag interaction. The classical eight-membered cage is formed by a nearly planar ring of [AgNCN]₂ sequence, where N-Ag distances fall in 2.1 to 2.2 Å, being in agreement with some Ag-N polymers recently described [27]. When compared to the crystal structure of sulfathiazole polymorphs I and II described in reference [28], the S-O distances in the silver complex (both 1.430 Å) remains unchanged. The bond distance between O2 (SO₂ group)...Ag(I) is longer than 3.0 Å, indicating a weak interaction between O2...Ag(I). On the other hand, the other oxygen atom of sulfonamide group is close to Ag(I) ion, with a distance 2.579 Å. So, a 1D polymer network along b axis can be generated, as described in Fig. 3. The Ag-SFT network also display H-bond between amine group of different asymmetric units with short distances falling in the range 2.60-2.91 Å, and π -stacking interaction of 3.448 Å between parallel phenyl rings also been observed. ESI #2 details those intermolecular interactions and shows the packing of Ag-SFT along [010].

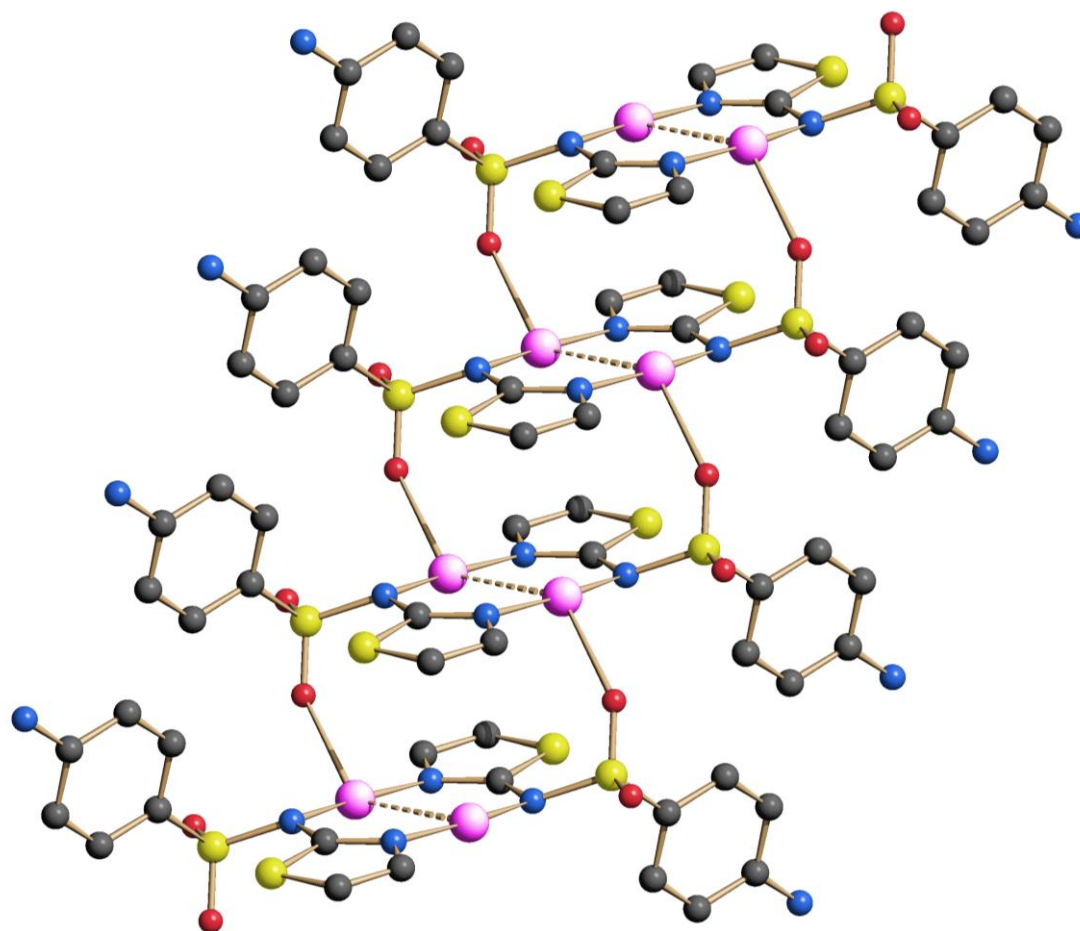


Fig. 3. The 1D Ag-SFT polymeric chain formed along b axis by the Ag-O bonding. Silver ions are colored as pink while nitrogen, oxygen, sulfur and carbon atoms are colored as blue, red, yellow and black, respectively and the hydrogen atoms were omitted for clarity. The dimer was generated applying 2-x,1-y,-z symmetry code and the 1D atoms were generated applying x,-1+y,z and x,-2+x,z symmetry codes.

Mass Spectrometric analyses

The mass spectrum of the Ag-SFT complex is presented in ESI #3. The peaks at m/z 362.0 and 364.0 correspond to the molecular ion $\text{AgC}_9\text{H}_8\text{N}_3\text{O}_2\text{S}_2$, which confirms the 1:1 metal/ligand composition, and the isotopic distribution of silver. The peak at m/z 256.1 corresponds to the free SFT. There are also other species at higher m/z values, which correspond to recombination of the ligand and silver(I) in solution. The MS-MS analysis shows the molecular ion with m/z 363.1 and the silver ion peak with m/z 108.5.

1 The mass spectrum of the Ag-SFM complex is presented in ESI #4. The peaks at
2 m/z 360.0 and 362.0 correspond to the molecular ion $\text{AgC}_{10}\text{H}_{10}\text{N}_3\text{O}_3\text{S}$. The peak with
3
4 m/z 254.1 corresponds to the free SFM. Other fragments at higher m/z were also
5
6 observed, which correspond to recombination of the ligand and silver(I) in solution as
7
8 described for the Ag-SFT complex. The MS-MS analysis shows the molecular ion with
9
10 m/z 360.0 and the silver ion peak with m/z 108.0.
11
12
13
14
15
16
17

18 *Vibrational Spectroscopy*

19
20
21 As described in the literature, the $\nu(\text{N-H})$ vibration bands of sulfonamides are
22
23 observed in the range $3320\text{-}3250\text{ cm}^{-1}$, while the sulphonyl group presents four different
24
25 bands, the $\nu_{\text{as}}(\text{O}=\text{S}=\text{O})$ around 1350 cm^{-1} , the $\nu_{\text{s}}(\text{O}=\text{S}=\text{O})$ at 1160 cm^{-1} , and the
26
27 scissoring and wagging deformation modes in the ranges $568\text{-}520$ and $529\text{-}487\text{ cm}^{-1}$,
28
29 respectively [29,30].
30
31
32
33

34 Both IR spectra of the silver sulfathiazole and silver sulfamethoxazole
35
36 complexes were reported earlier [18, 31]. The IR spectra of SFT, SFM and the
37
38 respective complexes here described are shown in Fig. 4. In the IR spectrum of SFT the
39
40 NH_2 stretching modes appear at 3354 and 3321 cm^{-1} , while in the IR spectrum of Ag-
41
42 SFT these bands appear at 3409 and 3339 cm^{-1} , respectively. The angular deformation
43
44 of (H-N-H) of the amino group appears at 1626 cm^{-1} for the SFT and at 1636 cm^{-1} for
45
46 the Ag-SFT complex. Regarding the four typical vibrational modes of the sulphonyl
47
48 group, for SFT the $\nu_{\text{as}}(\text{O}=\text{S}=\text{O})$ appears at 1323 cm^{-1} , the $\nu_{\text{s}}(\text{O}=\text{S}=\text{O})$ at 1140 cm^{-1} , and
49
50 the scissoring and wagging deformation modes at 555 and 507 cm^{-1} , respectively. For
51
52 Ag-SFT the $\nu_{\text{as}}(\text{O}=\text{S}=\text{O})$ appears at 1312 cm^{-1} , the $\nu_{\text{s}}(\text{O}=\text{S}=\text{O})$ at 1136 cm^{-1} , and the
53
54 scissoring and wagging deformation modes at 507 and 511 cm^{-1} . It is clear that the
55
56
57
58
59
60
61
62
63
64
65

vibrational modes of the sulfonyl group remain unchanged upon coordination, confirming the non-coordination of SFT to Ag(I) through the oxygen atoms of the sulfonamide, as seen by the crystal structure. Finally, the (C-N) stretching appears at 1497 cm^{-1} in the SFT spectrum and at 1502 cm^{-1} in the Ag-SFT one.

In the IR spectrum of SFM the NH_2 stretchings of the amino group appear at 3468 and 3379 cm^{-1} and the N-H stretching of the sulfonamide group appears at 3300 cm^{-1} . In the IR spectrum of Ag-SFM, the NH_2 stretching modes of the amino group appear at 3456 and 3389 cm^{-1} . The angular deformation of (H-N-H) of the amino group appears at 1622 cm^{-1} for the SFM and at 1616 cm^{-1} for the Ag-SFM complex. The four typical vibrational modes of the sulfonyl group appear in the free SFM and also in the complex: for SFM, the $\nu_{\text{as}}(\text{O}=\text{S}=\text{O})$ appears at 1313 cm^{-1} , the $\nu_{\text{s}}(\text{O}=\text{S}=\text{O})$ at 1144 cm^{-1} , and the scissoring and wagging deformation modes at 548 and 557 cm^{-1} , respectively. For Ag-SFM the $\nu_{\text{as}}(\text{O}=\text{S}=\text{O})$ appears at 1229 cm^{-1} , the $\nu_{\text{s}}(\text{O}=\text{S}=\text{O})$ at 1126 cm^{-1} , and the scissoring and wagging deformation modes at 509 and 523 cm^{-1} .

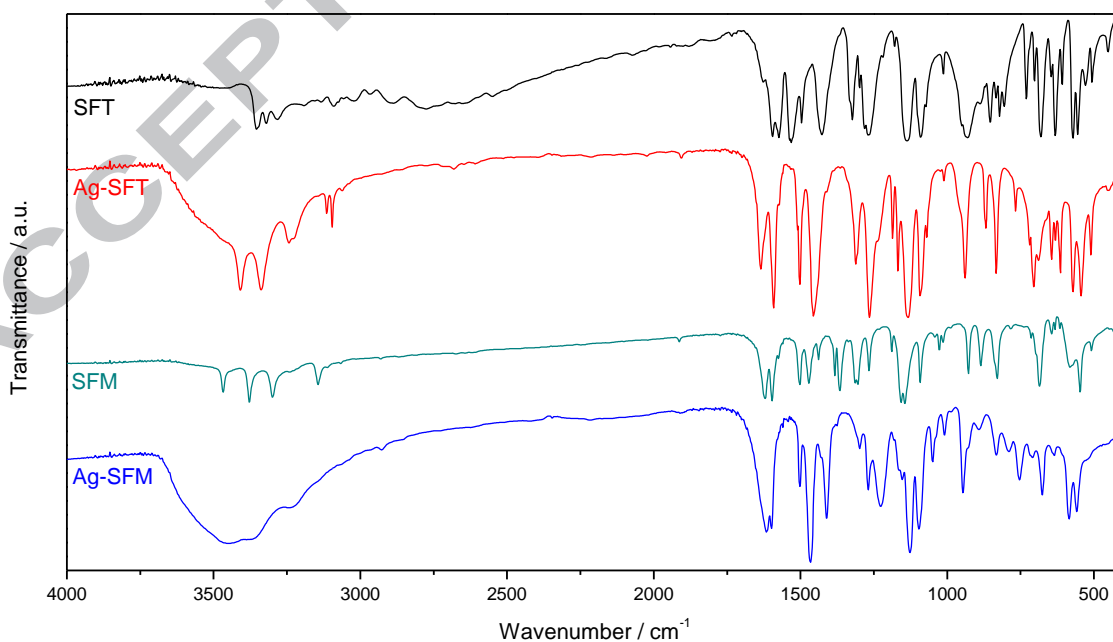


Fig. 4. Infrared vibrational spectra of sulfathiazole (SFT), Ag-SFT, sulfamethoxazole (SFM) and Ag-SFM.

Nuclear Magnetic Resonance Spectroscopy

Solution state ^1H , ^{13}C and $[^1\text{H}-^{15}\text{N}]$ heteronuclear multiple bond coherence (HMBC) NMR spectra were obtained in order to confirm the coordination sites of the sulfonamides to Ag(I). The NMR spectra of the Ag-SFT and Ag-SFM complexes were analyzed by a comparison to the NMR spectra of the free ligands. The structures of sulfathiazole and sulfamethoxazole with carbon assignments were already presented in Fig. 1.

Heteronuclear multiple bond coherence $[^1\text{H}-^{15}\text{N}]$ NMR spectroscopic measurements of samples with natural abundance of ^{15}N have been used successfully to evaluate the coordination of N-donor ligands to different metals [32 - 35]. The $[^1\text{H}-^{15}\text{N}]$ HMBC spectra are provided in Fig. 5. In the sulfathiazole spectrum the ^{15}N chemical shift of the nitrogen atom of the sulfonamide group is observed at 157.3 ppm, while in the Ag-SFT spectrum, this signal is observed at 223.2 ppm. The observed $\Delta\delta$ ($\delta_{\text{complex}} - \delta_{\text{ligand}}$) of 65.9 ppm confirms coordination of SFT to Ag(I) through the nitrogen atom of the sulfonamide group. On the other hand, the nitrogen atom of the NH_2 group appears at 69.1 ppm in the SFT spectrum, while for the complex it appears at 69.3 ppm. The minor chemical shift of 0.2 ppm when compared to the ^{15}N shift of the nitrogen of the sulfonamide group suggests that SFT is not coordinated to Ag(I) through the NH_2 group. The nitrogen of the thiazole group did not appear in the considered spectral window. For SFM the pattern is the same. The ^{15}N chemical shift of the nitrogen atom of the sulfonamide group is observed at 344.6 ppm, while in the Ag-SFM spectrum, this signal is observed at 302.0 ppm ($\Delta\delta = -42.6$ ppm). The nitrogen atom of the NH_2 group

appears at 71.3 ppm in the SFM spectrum and for the complex it appears at 77.3 ppm ($\Delta\delta$ of -4 ppm). The nitrogen of the thiazole group cannot be seen using [^1H - ^{15}N] HMBC due to the lack of coupling hydrogen atoms.

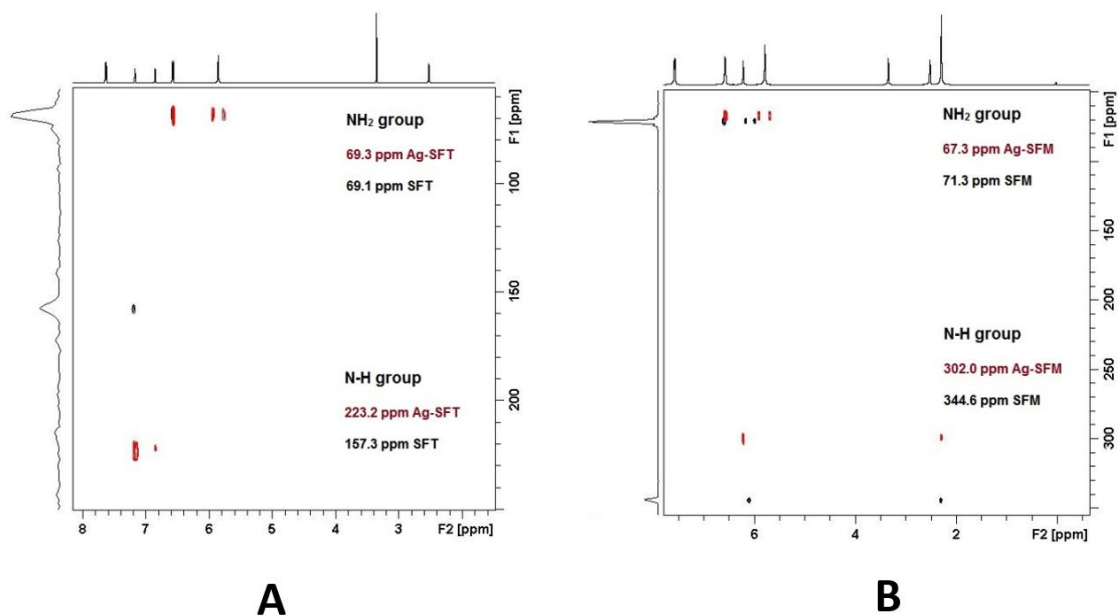


Fig. 5. [^1H - ^{15}N] NMR spectra of (A) SFT and Ag-SFT and (B) SFM and Ag-SFM. The external projections in both figures are the spectra of the corresponding complex.

Further information about the coordination sites of SFT and SFM were obtained by the evaluation of the solution state ^1H NMR spectra. The obtained spectra for both ligands and complexes are presented in Fig. 6, while the corresponding assignments and chemical shifts are presented in Table 3. The signals at 2.50 ppm and 3.30 ppm in all spectra are assigned to the CH_3 of DMSO and to HOD, respectively. For SFT, the hydrogen which appears as a singlet at 12.4 ppm in its ^1H NMR spectrum is no longer observed in the spectrum of the Ag-SFT complex. The same behavior is observed for SFM and for the Ag-SFM complex. This data lead us to consider the loss of the hydrogen atom of the ($\text{O}_2\text{S-N-H}$) group of the sulfonamides and nitrogen coordination to the metal center. This evidence, in addition to the expressive ^{15}N chemical shift of the

nitrogen atom of the (N–H) group when the ligand and the complex data are compared, confirms nitrogen coordination of the sulfonamide group to Ag(I) for both complexes.

The carbon chemical shifts and the carbon NMR spectrum for SFT and the Ag-SFT complex are presented in ESI #5, while the carbon chemical shifts and the carbon NMR spectrum for the SFM and the Ag-SFM complex are presented in ESI #6. For SFT and Ag-SFT the carbon atoms of the thiazol group are the most shifted, while for SFM and Ag-SFM the carbon next to the sulfur of the sulfonamide group is the most affected upon coordination, thus confirming the coordination sites of the ligands to Ag(I) as proposed previously by ^1H and [^1H - ^{15}N] HMBC NMR data.

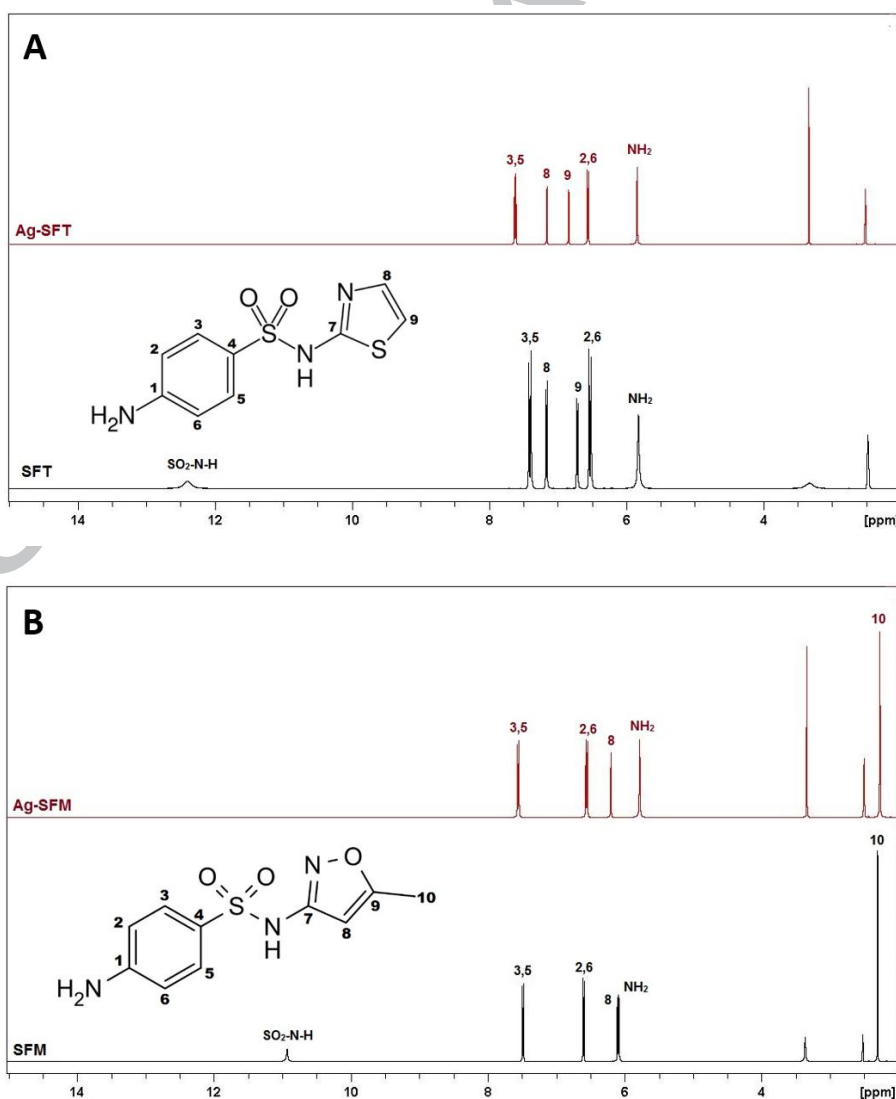


Fig. 6. ¹H NMR spectra of (A) SFT and Ag-SFT and (B) SFM and Ag-SFM in DMSO-d₆.**Table 3.** ¹H NMR assignments and chemical shifts for SFT and Ag-SFT, SFM and Ag-SFM.

Assignments	SFT	Ag-SFT	$\Delta\delta$ / ppm	Multiplicity	SFM	Ag-SFM	$\Delta\delta$ / ppm	Multiplicity
	δ / ppm	δ / ppm			δ / ppm	δ / ppm		
NH ₂	5.80	5.85	0.05	s	6.08	5.79	-0.29	s
2,6	6.51-6.55	6.55-6.57	0.03	d	6.58-6.60	6.56-6.58	-0.20	d
3,5	7.39-7.43	7.62-7.63	0.21	d	7.47-7.49	7.56-7.58	0.09	d
SO ₂ -N-H	12.40	-	-	s	10.93	-	-	s
8	7.16-7.18	7.16-7.17	-0.005	d	6.1	6.22	0.12	s
9	6.71-6.73	6.84-6.85	0.12	d	-	-	-	-
10	-	-	-	-	2.30	2.29	-0.01	s

Antibacterial Assays

The antibacterial activities of the Ag-SFT and Ag-SFM complexes were evaluated by the minimum inhibitory concentration (MIC) values. The selected bacterial strains include some of the most common pathogens responsible to colonize burn wounds, which are *S. aureus* (Gram-positive) and *P. aeruginosa* (Gram-negative) [36]. The results are presented in Table 4.

Table 4. Minimum inhibitory concentration (MIC) values of the antibacterial activities of the Ag-SFT and Ag-SFM complexes compared to pure SFT and SFM.

Compounds	Minimum inhibitory concentration (mmol L ⁻¹)		
	Gram-positive	Gram-negative	
	<i>S. aureus</i> ATCC 25923	<i>P. aeruginosa</i> ATCC 27853	<i>S. enterica</i> ATCC 10708
SFT	*	*	*
Ag-SFT	6.90	3.45	3.45
SFM	*	*	*
Ag-SFM	13.9	1.74	1.74

*Did not present inhibitory activity under the tested concentrations.

1
2
3
4
5
6
7
8
9
10
11
12
13
14
15
16
17
18
19
20
21
22
23
24
25
26
27
28
29
30
31
32
33
34
35
36
37
38
39
40
41
42
43
44
45
46
47
48
49
50
51
52
53
54
55
56
57
58
59
60
61
62
63
64
65

The MIC values for the Ag-SFT in DMSO solution show its antibacterial activity against both Gram-positive and Gram-negative strains. The MIC values were found at 3.45 mmol L⁻¹ for Gram-negative and 6.90 mmol L⁻¹ for Gram-positive strains. The MIC values for the Ag-SFM in DMSO solution also show its antibacterial activity against Gram-positive and Gram-negative strains, being 1.74 mmol L⁻¹ for Gram-negative and 13.9 mmol L⁻¹ for Gram-positive. The silver complexes were more active over Gram-negative strains. Free SFT and SFM did not show antibacterial activities in the same experimental conditions. The silver(I) complex with nimesulide, another sulfonamide, was also active against *E. coli* and *S. aureus* bacterial strains, as early reported [37]. A wide study regarding the antimicrobial activity of silver sulfadiazine, probably the most important silver-sulfonamide compound, was conducted over more than 400 strains including methicillin-resistant *S. aureus* and *Acinetobacter spp.* The MIC values were found in the range 44.8-179.2 μmol L⁻¹ [38]. The antibacterial activities observed for Ag-SFT and Ag-SFM complexes, in addition to their solubilities in DMSO, justifies further studies regarding the use of such compounds *in vivo* for the treatment of skin infections.

Conclusion

Molar composition of Ag-SFM and Ag-SFT complexes were found to be 1:1. Elemental, and mass spectrometric analyses confirm the coordination formulas [Ag(C₉H₈N₃O₂S₂)] for Ag-SFT complex and [Ag(C₁₀H₁₀N₃O₃S)] for Ag-SFM complex. The Ag-SFT and Ag-SFM compounds were shown to be soluble in DMSO. The ¹H-¹⁵N NMR data showed the coordination of the silver atom in both complexes through the nitrogen atom of the sulfonamide groups of the ligands. The crystal structure of Ag-SFT

1 was solved by power X-ray diffraction and point to a dimeric arrangement with silver(I)
2 ions bridging between two ligands. Coordination of SFT to Ag(I) occurs through the
3
4 nitrogen atoms of the sulfonamide and thiazole groups. The Ag-SFT and Ag-SFM
5
6 complexes were also tested against Gram-positive and Gram-negative bacteria in
7
8 DMSO solutions. The MIC values for the Ag-SFT show its antibacterial activity against
9
10 both Gram-positive and Gram-negative bacteria in the range 3.45-6.90 mmol L⁻¹, while
11
12 for the Ag-SFM complex the MIC values were in the range 1.74-13.9 mmol L⁻¹. In all
13
14 cases, the complexes were shown to be more active against Gram-negative strains.
15
16
17
18
19
20
21

22 **Crystallographic data**

23
24
25 Crystal data, fractional atomic coordinates and displacement parameters of the
26
27 Ag-SFT structure described in this paper are supplied in standard CIF deposited at the
28
29 Cambridge Crystallographic Data Centre (1012190). The data can be obtained free of
30
31 charge at <http://www.ccdc.cam.ac.uk/conts/retrieving.html> [or from Cambridge
32
33 Crystallographic Data Centre (CCDC), 12 Union Road, Cambridge CB2 1EZ, UK; fax:
34
35 +44 (0) 1223-336033; e-mail: deposit@ccdc.cam.ac.uk].
36
37
38
39
40
41
42

43 **Acknowledgements**

44
45 This study was supported by grants from FAPESP (Fundação de Amparo à
46
47 Pesquisa do Estado de São Paulo, proc. n° 2012/08230-2), CNPq (Conselho Nacional de
48
49 Desenvolvimento Científico e Tecnológico, proc. n° 240094/2012-3) and FAPEMIG
50
51 (Fundação de Amparo à Pesquisa do Estado de Minas Gerais, proc. n° CEX-APQ-
52
53 00525/14).
54
55
56
57
58
59
60
61
62
63
64
65

References

- 1
2
3
4 [1] H. J. Klasen, **Burns** 26 (2000) 117-130.
5
6
7 [2] B.S. Atiyeh, M. Costagliola, S.N. Hayek, S.A. Dibo, **Burns** 33 (2007) 139-148.
8
9
10 [3] S.M. Modak, C.L. Fox Jr., **Biochem. Pharmacol.** 22 (1973) 2391-2404.
11
12 [4] M. Solioz, A. Odermatt, **J. Biol. Chem.** 270 (1995) 9217-9221.
13
14 [5] K.M. Hindi, A.J. Ditto, M.J. Panzner, D.A. Medvetz, D.S. Han, C.E. Hovis, J.K.
15 Hilliard, J.B. Taylor, Y.H. Yun, C.L. Cannon and W.J. Youngs, **Biomaterials** 30
16 (2009) 3771-3779.
17
18
19
20 [6] D.G. Greenhalgh, **Clin. Plast. Surg.** 36 (2009) 597-606.
21
22
23 [7] K. Nomiya and H. Yokoyama, **Dalton Trans.** (2002) 2483-2490.
24
25
26 [8] S. Eckhardt, P.S. Brunetto, J. Gagnon, M. Priebe, B. Giese, K.M. Fromm,
27 **Chem. Rev.** 113 (2013) 4708-4754.
28
29 [9] L. Kyros, C. N. Banti, N. Kourkoumelis, M. Kubicki, I. Sainis, S. K. Hadjikakou
30 **J. Biol. Inorg. Chem.** (2014) 19, 449-464
31
32 [10] E. Kremer, G. Facchin, E. Estèves , P. Alborés, E.J. Baran, J. Ellena, M.H. Torre
33 **J. Inorg. Biochem.** 100 (2006) 1167-1175.
34
35 [11] W. Baran, E. Adamek, J. Ziemianska, A. Sobczak, **J. Haz. Mat.** 196 (2011) 1-
36 15.
37
38 [12] R.E.F. de Paiva, C. Abbehausen, A.F. Gomes, F.C. Gozzo, W.R. Lustri, A.L.B.
39 Formiga, P.P. Corbi; **Polyhedron** 36 (2012) 112-119.
40
41 [13] C.L. Fox, B.W. Rappole, W. Stanford, **Surg. Gynecol. Obstet.** 128 (1969)
42 1021-1026.
43
44
45
46
47
48
49
50
51
52
53
54
55
56
57
58
59
60
61
62
63
64
65

- [14] E. Scholar, **xPharm: The Comprehensive Pharmacology Reference**, 2009, Elsevier, New York, pages 1-3.
- [15] G.M. Golzar Hossain, **J. Saudi Chem. Soc.** (2013) 17, 253-257.
- [16] S. Bellú, E. Hure, M. Trapé, C. Trossero, G. Molina, C. Drogo, P.A.M. Williams, A.M. Atria, J.C.M. Acevedo, S. Zacchino, M. Sortino, D. Campagnoli, M. Rizzotto, **Polyhedron** 24 (2005) 501-509.
- [17] W. Henderson, L.J. McCaffrey, M.B. Dinger, B.K. Nicholson, **Polyhedron** 17 (18) (1998) 3137-3144.
- [18] K.K. Narang, J.K. Gupta, **Curr. Sci.** 45 (1976) 744-746.
- [19] N. Absar, H. Daneshvar, G. Beall, **J. Allergy Clin. Immunol.** 93 (6) (1994) 1001-1005.
- [20] M. Mondelli, F. Pavan, P.C. de Souza, C.Q. Leite, J. Ellena, O.R. Nascimento, G. Facchin, M.H. Torre, **J. Mol. Struct.** 1036 (2013) 180-187.
- [21] B. Kesimli, A. Topacli, **Spectrochim. Acta Part A** 57 (2001) 1031-1036.
- [22] L.L. Marques, G.M. de Oliveira, E.S. Lang, M.M.A. de Campos, L.R.S. Gris, **Inorg. Chem. Commun.** 10 (2007) 1083-1087.
- [23] Clinical and Laboratory Standards Institute (CLSI), **Performance Standards for Antimicrobial Susceptibility Testing**, 17th Informational Supplement, Wayne, PA, USA, 2007.
- [24] E. Keller, **Chem. Unserer Zeit** 20 (1986) 178-181.
- [25] I.M.P. Silva, D.M. Profirio, R.E.F. de Paiva, M. Lancellotti, A.L.B. Formiga, P.P. Corbi, **J. Mol. Struct.** 1049 (2013) 1-6.
- [26] A. Cuin, A.C. Massabni, C.Q.F. Leite, D.N. Sato, A. Neves, B. Szpoganicz, M.S. Silva, A.J. Bortoluzzi, **J. Inorg. Biochem.** 101 (2007) 291-296.

- 1 [27] S.A. da Silva, C.Q.F. Leite, F.R. Pavan, N. Masciocchi, A. Cuin, **Polyhedron** 79
2
3 (2014) 170–177.
4
5 [28] T.N. Drebuschak, E.V. Boldyreva, M.A. Mikhailenko, **J. Struct. Chem.** 49
6
7 (2008) 84-94.
8
9 [29] J.N. Baxter, J. Cymerman-Craig, J.B. Willis, **J. Chem. Soc.** (1955) 669-679.
10
11 [30] M. Goldstein, M.A. Russell, H.A. Willis, **Spectrochim. Acta A** 25 (7) (1969)
12
13 1275-1285.
14
15 [31] S. P. Vijaya Chamundeeswari, E. James Jebaseelan Samuel, N. Sundaraganesan,
16
17 **Spectrochim. Acta A** 118 (2014) 1-10.
18
19 [32] N. Juranic, S. Macura, **Inorg. Chim. Acta** 217 (1994) 213-215.
20
21 [33] P.P. Corbi, A.C. Massabni, T.A. Heinrich, C.M. Costa-Neto, **J. Coord. Chem.**
22
23 61 (2008) 2470-2477.
24
25 [34] P.P. Corbi, A.C. Massabni, **Spectrochim. Acta A** 64 (2006) 418-419.
26
27 [35] C. Abbehausen, J.F. Castro, M.B.M. Spera, T.A. Heinrich, C.M. Costa-Neto,
28
29 W.R. Lustri, A.L.B. Formiga, P.P. Corbi, **Polyhedron** 30 (2011) 2354-2359.
30
31 [36] S. Erol, U. Altoparlak, M.N. Akcay, F. Celebi, M. Parlak, **Burns** 30 (2004) 357-
32
33 361.
34
35 [37] R.E.F. de Paiva, C. Abbehausen, F.R.G. Bergamini, A.L. Thompson, D.A.
36
37 Alves, M. Lancellotti, P.P. Corbi, **J. Incl. Phenom. Macro. Chem.** 79 (2014)
38
39 225-235.
40
41 [38] J.M.T. Hamilton-Miller, S. Shah, C. Smith, **Chemotherapy** 39 (1993) 405-409.
42
43
44
45
46
47
48
49
50
51
52
53
54
55
56
57
58
59
60
61
62
63
64
65

Figure Captions List

Fig. 1. Sulfathiazole (**A**) and sulfamethoxazole (**B**) structures with carbon numbering.

The four torsion angles used in the powder diffraction studies were assigned in the SFT drawn.

Fig. 2. Schakal [24] drawn of dimeric Ag-SFT. The atoms of the asymmetric unit of Ag-SFT are numbered and the symmetry code 2-x, 1-y, -z was applied to generate the dimer form. Silver is colored as pink; nitrogen, oxygen, sulfur, carbon and hydrogen atoms are colored as blue, red, yellow, black and white, respectively.

Fig. 3. The 1D Ag-SFT polymeric chain formed along b axis by the Ag-O bonding. Silver ions are colored as pink while nitrogen, oxygen, sulfur and carbon atoms are colored as blue, red, yellow and black, respectively and the hydrogen atoms were omitted for clarity. The dimer was generated applying 2-x,1-y,-z symmetry code and the 1D atoms were generated applying x,-1+y,z and x,-2+x,z symmetry codes.

Fig. 4. Infrared vibrational spectra of sulfathiazole (SFT), Ag-SFT, sulfamethoxazole (SFM) and Ag-SFM.

Fig. 5. [^1H - ^{15}N] NMR spectra of (**A**) SFT and Ag-SFT and (**B**) SFM and Ag-SFM. The external projections in both figures are the spectra of the corresponding complex.

Fig. 6. ^1H NMR spectra of (**A**) SFT and Ag-SFT and (**B**) SFM and Ag-SFM, in DMSO-d₆.

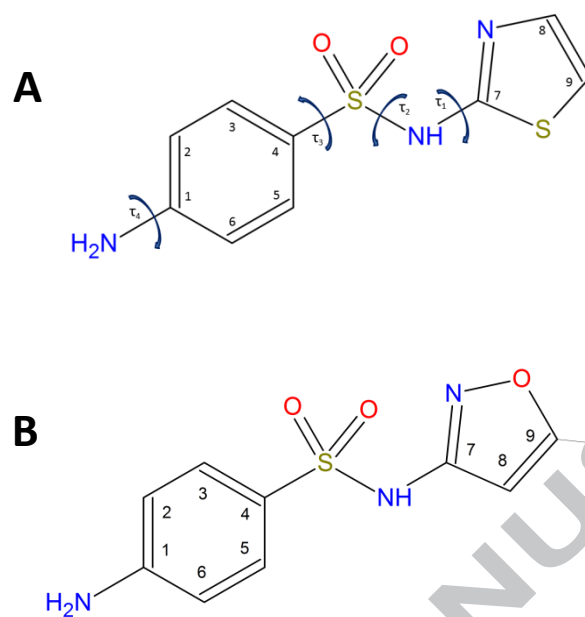


Fig. 1. Sulfathiazole (A) and sulfamethoxazole (B) structures with carbon numbering. The four torsion angles used in the powder diffraction studies were assigned in the SFT drawn.

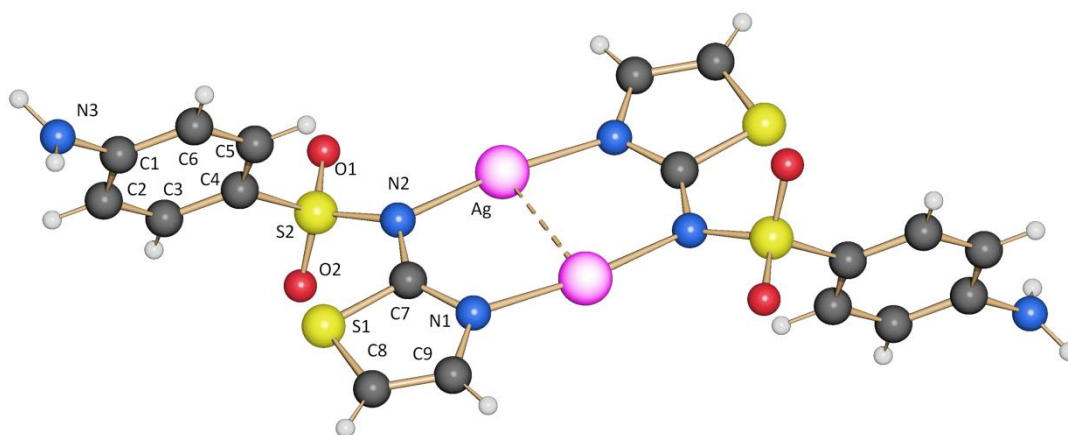


Fig. 2. Schakal [24] drawn of dimeric Ag-SFT. The atoms of the asymmetric unit of Ag-SFT are numbered and the symmetry code $2-x, 1-y, -z$ was applied to generate the dimer form. Silver is colored as pink; nitrogen, oxygen, sulfur, carbon and hydrogen atoms are colored as blue, red, yellow, black and white, respectively.

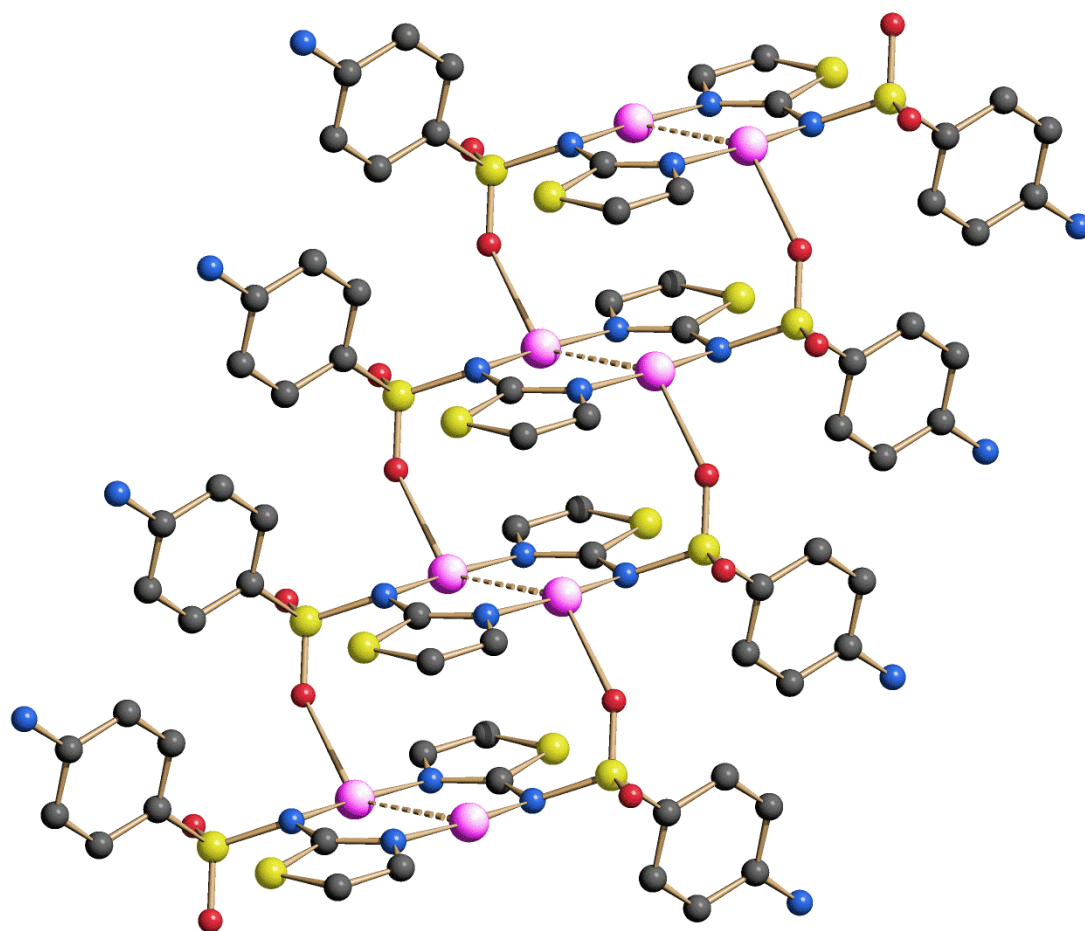


Fig. 3. The 1D Ag-SFT polymeric chain formed along b axis by the Ag-O bonding. Silver ions are colored as pink while nitrogen, oxygen, sulfur and carbon atoms are colored as blue, red, yellow and black, respectively and the hydrogen atoms were omitted for clarity. The dimer was generated applying $2-x, 1-y, -z$ symmetry code and the 1D atoms were generated applying $x, -1+y, z$ and $x, -2+x, z$ symmetry codes.

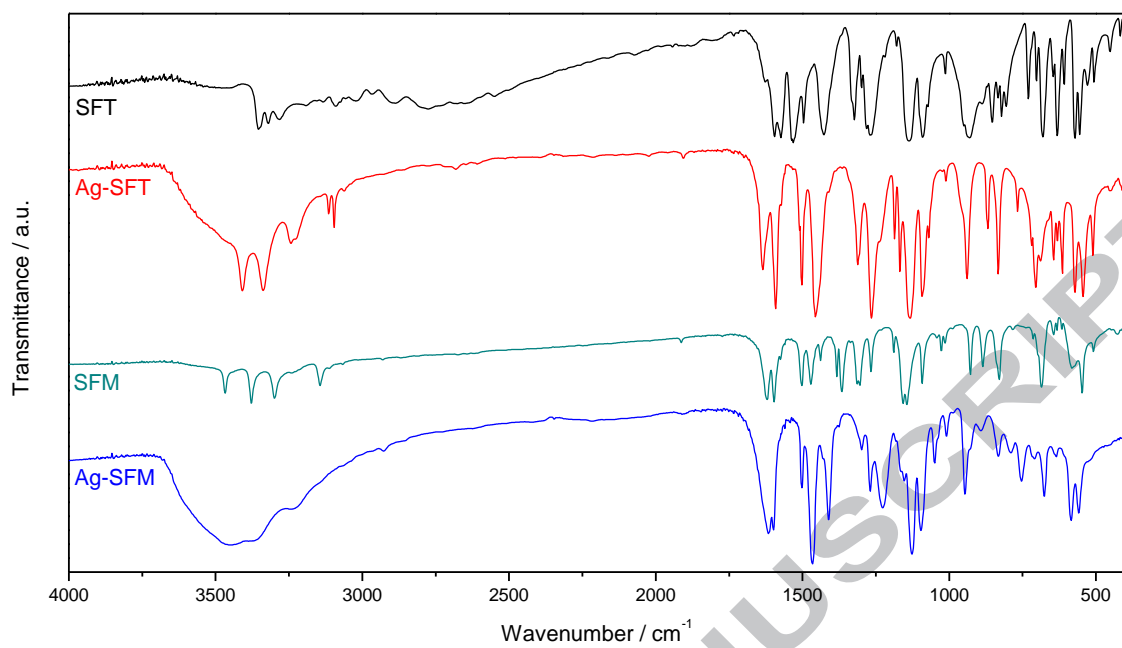


Fig. 4. Infrared vibrational spectra of sulfathiazole (SFT), Ag-SFT, sulfamethoxazole (SFM) and Ag-SFM.

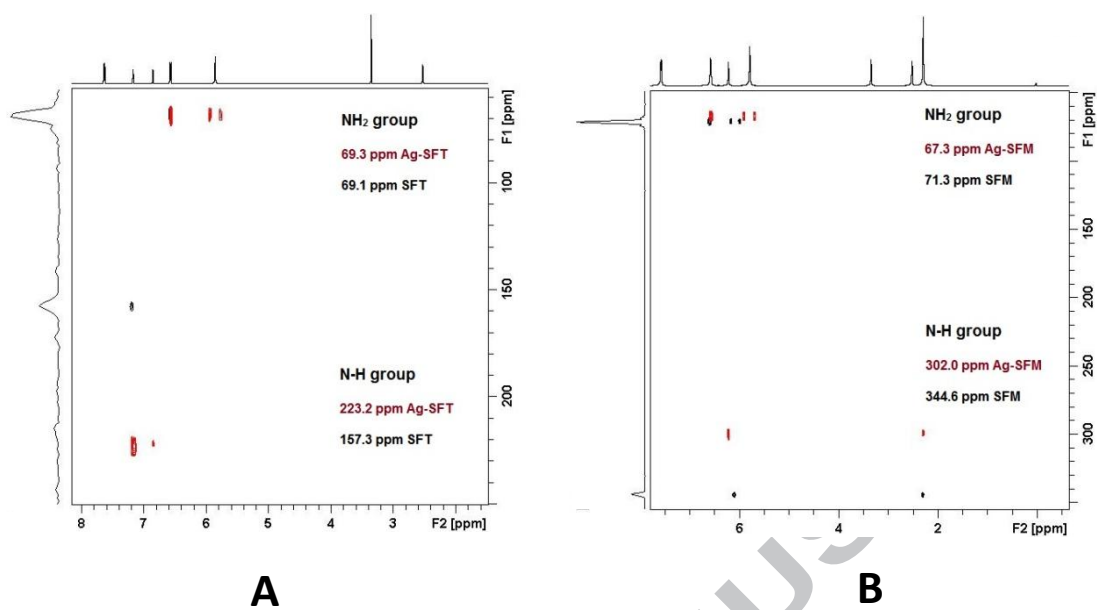


Fig. 5 [¹H-¹⁵N] NMR spectra of (A) SFT and Ag-SFT and (B) SFM and Ag-SFM. The external projections in both figures are the spectra of the corresponding complex.

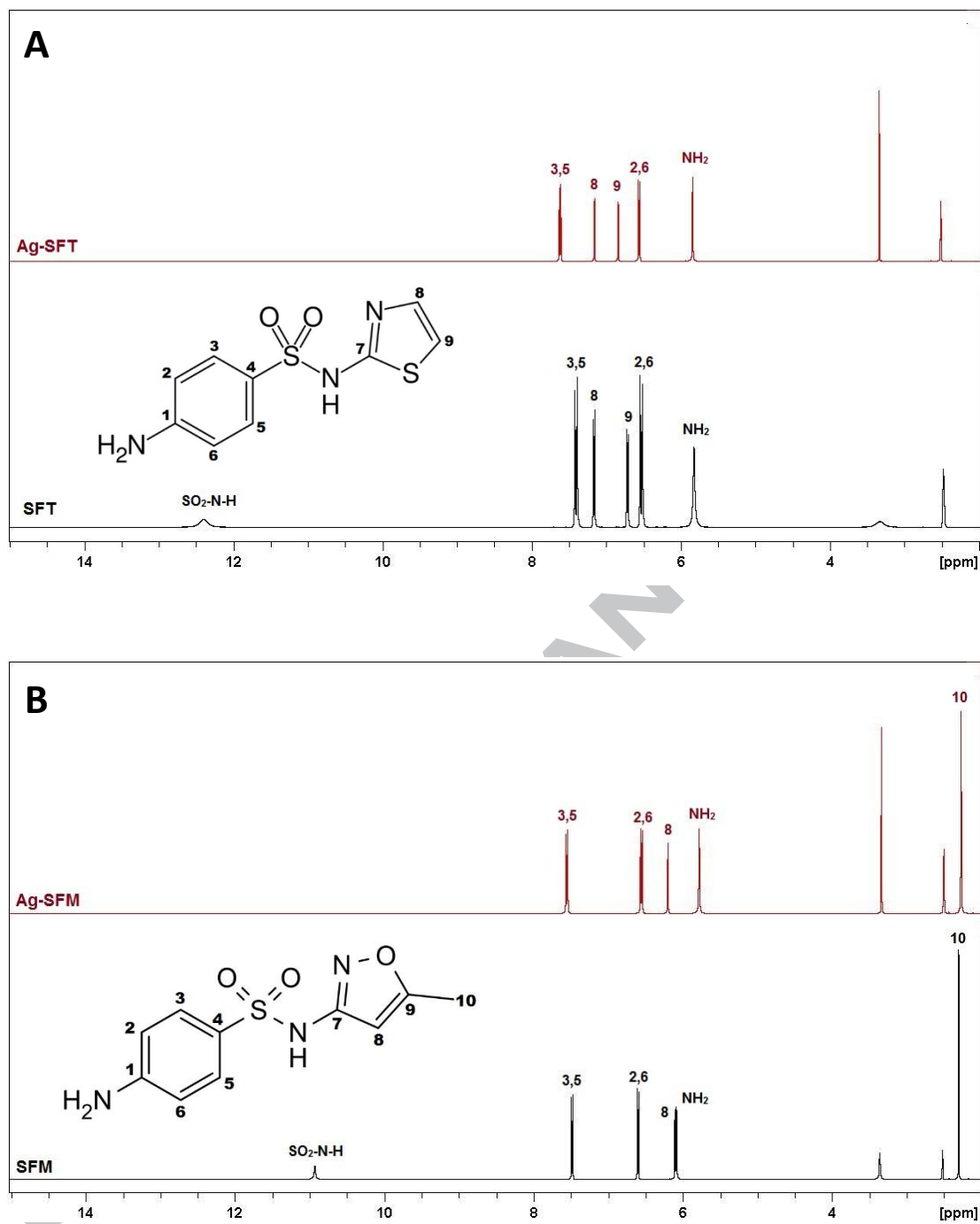


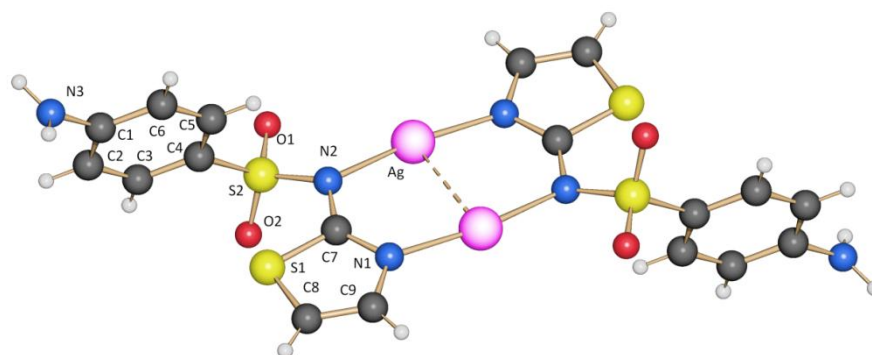
Fig. 6. ¹H NMR spectra of (A) SFT and Ag-SFT and (B) SFM and Ag-SFM, in DMSO-d₆.

Graphical Abstract Synopsis

Structure of the silver complex with sulfathiazole obtained by powder X-ray crystallographic studies

ACCEPTED MANUSCRIPT

Graphical Abstract



Structure of the silver complex with sulfathiazole obtained by powder X-ray crystallographic studies

ACCEPTED MANUSCRIPT